Modeling of QMS with Pendulum Attachment

1 System Description

The Quanser Motion System (QMS) comes with two motor-load attachments; an inertia disk (resulting in 2nd-order dynamics) and a pendulum (resulting in 4th-order dynamics). A detailed model of the QMS with pendulum attachment is provided in this document.

A physics-based model of the plant must be available before a model-based controller design can be pursued, and such a modeling effort requires a clear description of the physical system under investigation. To this end, schematic diagrams displaying our system's main mechanical elements are shown in Figure 1; the 1st axis has rotary motion, whereas the 2nd axis is a pendulum.

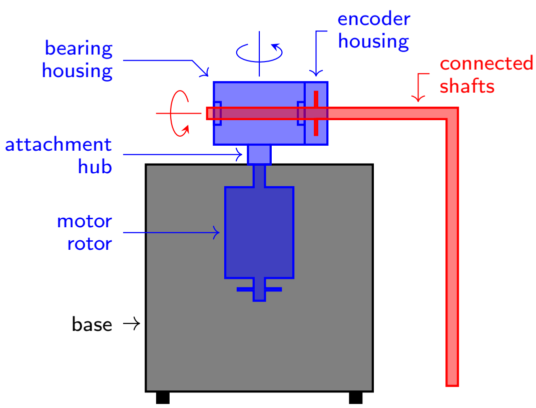

(a) Fabrication perspective.

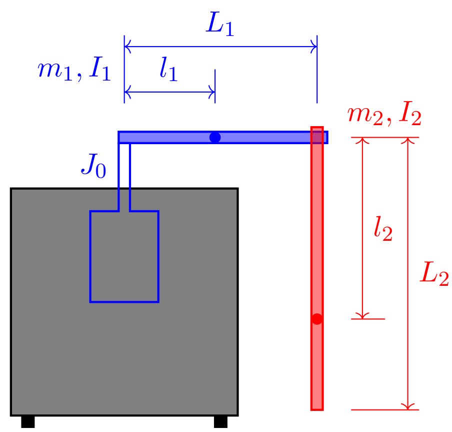

(b) Modeling perspective.

Figure 1: Schematic diagrams of the QMS with pendulum attachment.

Figure 1a reveals details of how the system is constructed from three subsystems. A stationary base (black) houses a motor, a power converter, a microcontroller, and a connector for two-way serial communication. This microcontroller enables the serial communication, interfaces with the power converter to impose motor voltage and measure motor current, and interfaces with optical encoders to measure angular positions; motion control is the responsibility of our external microcontroller, with commands and measurements conveyed as serial data packets. A first assembly (blue) rotates about a vertical axis and consists of the first encoder's disk, the motor's rotor, an attachment hub, a bearing housing, and the second encoder's housing. A second assembly (red) rotates about a horizontal axis and consists of a first shaft supported by the bearing housing, the second encoder's disk, and a connected second shaft that is perpendicular to the first shaft.

Figure 1b declares the parameters needed to develop a physics-based model of the system. In this representation, link 0 (blue outline) is the torque-transmission mechanism, link 1 (blue) is the horizontal shaft, link 2 (red) is the vertical shaft, and link 0 is rigidly attached to link 1. Link 0 has inertia J_0 with respect to the rotation axis. Link 1 has length L_1, center of mass at distance l_1 from the rotation axis, mass m_1, and inertia I_1 with respect to the center of mass. Link 2 has length L_2, center of mass at distance l_2 from the rotation axis, mass m_2, and inertia I_2 with respect to the center of mass. These parameters are sufficient for developing the equations of motion.

Figure 2 defines link angles, θ_1 and θ_2, relative to reference angles (dashed lines). The equations of motion are influenced by the reference angle defining θ_2 (see Figure 2b), but not by the reference angle defining θ_1 (see Figure 2a). Nevertheless, both reference angles are relevant and must be understood when performing experiments, because the system uses relative encoders rather than absolute encoders. Furthermore, in the experimental system, hard stops are present to limit the rotation range of link 1 as illustrated by the arc imprinted on the top of the base, and the reference angle defining θ_1 corresponds to the center of that arc.

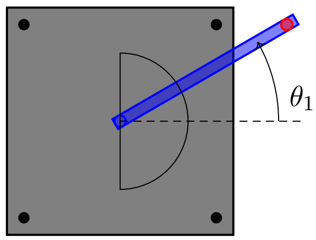

(a) Top view defining θ_1.

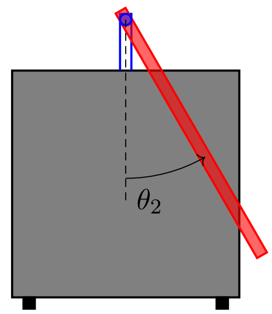

(b) Side view defining θ_2.

Figure 2: Reference definitions for angle measurements.

Before addressing the topic of mechanical dynamics in detail, it is appropriate to recognize that plant models might use either motor torque or motor voltage as the control input. A torque input assumption is valid only if a current regulator is employed. Our system does not include an internal current regulator. We could implement current regulation using our external microcontroller, but this is not necessary. Recall from lecture notes that torque τ and current i are related by

$$\tau = K_m i$$

where K_m is the motor's magnetic-coupling coefficient, and that voltage v influences current by

$$L_m \frac{di}{dt} = v - R_m i - K_m \dot{\theta}_m$$

where $\dot{\theta}_m$ is the motor's angular velocity, R_m is the motor's resistance, and L_m is the motor's inductance. Our system's motor uses core-less technology, which leads to a combination of small inductance (1.16 mH) and large resistance (8.4 Ω), and thus an electrical time constant of just 138 μs. Therefore, for our motor it is possible to accurately relate torque and voltage directly, by setting $L_m = 0$ above and solving for i, resulting in the algebraic torque-voltage relation

$$\tau = K_m i = \frac{K_m}{R_m}\left(v - K_m \dot{\theta}_1\right). \tag{1}$$

In this expression, we have substituted $\dot{\theta}_m = \dot{\theta}_1$, which is a consequence of a gearless direct-drive connection between the motor and link 1.

2 Nonlinear Model in Second-Derivative Form

A systematic method for deriving the equations of motion, called Lagrangian Dynamics, begins with the derivation of expressions for kinetic energy and potential energy (see lecture notes). Our system has two rotational axes, so we denote the vectors of two link angular positions and two link angular velocities by

$$\theta = \begin{bmatrix} \theta_1 \\ \theta_2 \end{bmatrix}, \quad \dot{\theta} = \begin{bmatrix} \dot{\theta}_1 \\ \dot{\theta}_2 \end{bmatrix}.$$

The scalar Lagrangian function $\mathcal{L}(\theta, \dot{\theta})$ is defined as the difference between kinetic energy, which depends on both θ and $\dot{\theta}$, and potential energy, which depends only on θ:

$$\mathcal{L}(\theta, \dot{\theta}) = E_{\text{kinetic}}(\theta, \dot{\theta}) - E_{\text{potential}}(\theta).$$

The equations of motion are determined from $\mathcal{L}(\theta, \dot{\theta})$ by evaluating Lagrange's equations

$$\frac{d}{dt}\left\{\frac{\partial \mathcal{L}}{\partial \dot{\theta}_i}\right\} - \frac{\partial \mathcal{L}}{\partial \theta_i} = \mu_i, \quad i \in \{1, 2\}$$

where torques μ_i account for extraction and/or insertion of energy. Our system has viscous friction with coefficients d_1 and d_2 at joints 1 and 2, and motor torque τ is applied at joint 1, so

$$\mu_1 = -d_1\dot{\theta}_1 + \tau, \quad \mu_2 = -d_2\dot{\theta}_2.$$

Application of this method leads to the nonlinear model

$$\mathcal{M}(\theta)\ddot{\theta} + \mathcal{V}(\theta, \dot{\theta}) + \mathcal{G}(\theta) = -\mathcal{D}\dot{\theta} + \mathcal{B}\tau \tag{2}$$

where the inertia matrix function $\mathcal{M}(\theta)$, the velocity-dependent torque vector function $\mathcal{V}(\theta, \dot{\theta})$, the gravity-dependent torque vector function $\mathcal{G}(\theta)$, the viscous friction coefficient matrix $\mathcal{D}$, and the actuator influence coefficient vector $\mathcal{B}$ are found to be

$$\begin{aligned}
\mathcal{M}(\theta) &= \begin{bmatrix} J_0 + J_1 + m_2L_1^2 + J_2\sin^2\theta_2 & m_2L_1l_2\cos\theta_2 \\ m_2L_1l_2\cos\theta_2 & J_2 \end{bmatrix} \\
\mathcal{V}(\theta, \dot{\theta}) &= \begin{bmatrix} -m_2L_1l_2\dot{\theta}_2^2\sin\theta_2 + 2J_2\dot{\theta}_1\dot{\theta}_2\sin\theta_2\cos\theta_2 \\ -J_2\dot{\theta}_1^2\sin\theta_2\cos\theta_2 \end{bmatrix} \\
\mathcal{G}(\theta) &= \begin{bmatrix} 0 \\ m_2gl_2\sin\theta_2 \end{bmatrix} \\
\mathcal{D} &= \begin{bmatrix} d_1 & 0 \\ 0 & d_2 \end{bmatrix} \\
\mathcal{B} &= \begin{bmatrix} 1 \\ 0 \end{bmatrix}
\end{aligned}$$

and where the inertias of links 1 and 2 have been restated relative to the rotation axes:

$$J_1 = I_1 + m_1l_1^2, \quad J_2 = I_2 + m_2l_2^2.$$

All of the above model coefficients are defined in Figures 1–2 except for d_1 and d_2 which have been added to approximate friction arising from the motor's commutator and the support bearings.

3 Linear Model in Second-Derivative Form

In this course, we have focused on stabilization of linear plants using linear controllers. What happens if we attempt instead to stabilize a nonlinear plant using a linear controller? Fortunately, for many applications, the controller is expected to keep plant state variables within a region of the state space on which the plant nonlinearities do not vary significantly. In such a situation, the plant nonlinearities can be well represented by truncated Taylor series approximations, leading to a linear approximate plant model. To construct such a model, we select the plant equilibrium point that the controller will need to stabilize. From (2), we see that no motion occurs, and hence our plant is at equilibrium, provided that

$$\begin{bmatrix} 0 \\ m_2 g l_2 \sin\theta_{2,\text{eq}} \end{bmatrix} = \begin{bmatrix} 1 \\ 0 \end{bmatrix} \tau_{\text{eq}}.$$

These equilibrium constraints further imply that all plant equilibrium points must satisfy

$$\tau_{\text{eq}} = 0, \quad \theta_{1,\text{eq}} = \text{unconstrained}, \quad \theta_{2,\text{eq}} = \begin{cases} \pi & \text{, pendulum points up} \\ 0 & \text{, pendulum points down.} \end{cases}$$

Given any of these plant equilibrium points that we wish to stabilize using a controller, (2) implies that the corresponding linear approximate plant model will require an order-0 Taylor series truncation of nonlinear function $\mathcal{M}(\theta)$ and order-1 Taylor series truncations of nonlinear functions $\mathcal{V}(\theta, \dot{\theta})$ and $\mathcal{G}(\theta)$. Since the linear approximate plant model is valid in a neighborhood of a specific plant equilibrium point, it follows that the state variables of the linear approximate plant model will be deviations from that specific plant equilibrium point, defined as

$$\vartheta_1 = \theta_1 - \theta_{1,\text{eq}}, \quad \vartheta_2 = \theta_2 - \theta_{2,\text{eq}}, \quad \dot{\vartheta}_1 = \dot{\theta}_1 - 0, \quad \dot{\vartheta}_2 = \dot{\theta}_2 - 0.$$

Using these deviation variables, (2) yields a linear approximate plant model of the form

$$\begin{bmatrix} J_{11} & \mp J_{12} \\ \mp J_{21} & J_{22} \end{bmatrix} \begin{bmatrix} \ddot{\vartheta}_1 \\ \ddot{\vartheta}_2 \end{bmatrix} + \begin{bmatrix} d_1 & 0 \\ 0 & d_2 \end{bmatrix} \begin{bmatrix} \dot{\vartheta}_1 \\ \dot{\vartheta}_2 \end{bmatrix} + \begin{bmatrix} 0 & 0 \\ 0 & \mp T_{22} \end{bmatrix} \begin{bmatrix} \vartheta_1 \\ \vartheta_2 \end{bmatrix} = \begin{bmatrix} 1 \\ 0 \end{bmatrix} \tau \tag{3}$$

where the new constant inertia and torque coefficients are found to be

$$J_{11} = J_0 + J_1 + m_2 L_1^2, \quad J_{12} = J_{21} = m_2 L_1 l_2, \quad J_{22} = J_2, \quad T_{22} = m_2 g l_2$$

and the signs correspond to the two possible values of $\theta_{2,\text{eq}}$; the upper sign applies if the pendulum is pointing up, and the lower sign applies if the pendulum is pointing down.

4 Linear Model in State-Space Form

It is now possible to write down the linear approximate plant model in state-space form, which is the point of departure for controller design. There are four possible state-space models, because the control input could be torque or voltage and the equilibrium could be pendulum-up or pendulum-down. The state variables are assigned in terms of deviations as

$$x_1(t) = \vartheta_1(t), \quad x_2(t) = \vartheta_2(t), \quad x_3(t) = \dot{\vartheta}_1(t), \quad x_4(t) = \dot{\vartheta}_2(t),$$

the output variables are assigned in terms of deviations as

$$y_1(t) = \vartheta_1(t), \quad y_2(t) = \vartheta_2(t),$$

and the input variable is assigned as

$$u(t) = \begin{cases} \tau(t) & \text{, if torque is control input} \\ v(t) & \text{, if voltage is control input.} \end{cases}$$

For the case of *torque* control input, (3) yields the linear approximate plant model

$$\dot{x}(t) = Fx(t) + Gu(t) \tag{4}$$

$$y(t) = Hx(t) \tag{5}$$

where the coefficient matrices have the form

$$F = \begin{bmatrix} 0 & 0 & 1 & 0 \\ 0 & 0 & 0 & 1 \\ 0 & f_{32} & f_{33} & f_{34} \\ 0 & f_{42} & f_{43} & f_{44} \end{bmatrix}, \quad G = \begin{bmatrix} 0 \\ 0 \\ g_3 \\ g_4 \end{bmatrix}, \quad H = \begin{bmatrix} 1 & 0 & 0 & 0 \\ 0 & 1 & 0 & 0 \end{bmatrix}$$

and the non-trivial submatrices are found to be

$$\begin{bmatrix} f_{32} & f_{33} & f_{34} \\ f_{42} & f_{43} & f_{44} \end{bmatrix} = \frac{1}{J_{11}J_{22} - J_{12}J_{21}} \begin{bmatrix} J_{12}T_{22} & -J_{22}d_1 & \mp J_{12}d_2 \\ \pm J_{11}T_{22} & \mp J_{21}d_1 & -J_{11}d_2 \end{bmatrix}$$

$$\begin{bmatrix} g_3 \\ g_4 \end{bmatrix} = \frac{1}{J_{11}J_{22} - J_{12}J_{21}} \begin{bmatrix} J_{22} \\ \pm J_{21} \end{bmatrix}.$$

For the case of *voltage* control input, (3) with (1) yields the linear approximate plant model

$$\dot{x}(t) = Ax(t) + Bu(t) \tag{6}$$

$$y(t) = Cx(t) \tag{7}$$

where the coefficient matrices have the form

$$A = \begin{bmatrix} 0 & 0 & 1 & 0 \\ 0 & 0 & 0 & 1 \\ 0 & a_{32} & a_{33} & a_{34} \\ 0 & a_{42} & a_{43} & a_{44} \end{bmatrix}, \quad B = \begin{bmatrix} 0 \\ 0 \\ b_3 \\ b_4 \end{bmatrix}, \quad C = \begin{bmatrix} 1 & 0 & 0 & 0 \\ 0 & 1 & 0 & 0 \end{bmatrix}$$

and the non-trivial submatrices are found to be

$$\begin{bmatrix} a_{32} & a_{33} & a_{34} \\ a_{42} & a_{43} & a_{44} \end{bmatrix} = \frac{1}{J_{11}J_{22} - J_{12}J_{21}} \begin{bmatrix} J_{12}T_{22} & -J_{22}\left(K_m^2/R_m + d_1\right) & \mp J_{12}d_2 \\ \pm J_{11}T_{22} & \mp J_{21}\left(K_m^2/R_m + d_1\right) & -J_{11}d_2 \end{bmatrix}$$

$$\begin{bmatrix} b_3 \\ b_4 \end{bmatrix} = \frac{1}{J_{11}J_{22} - J_{12}J_{21}} \begin{bmatrix} J_{22}K_m/R_m \\ \pm J_{21}K_m/R_m \end{bmatrix}.$$

For coefficient matrices, the signs correspond to the possible values of $\theta_{2,\text{eq}}$; the upper sign applies if the pendulum is pointing up, and the lower sign applies if the pendulum is pointing down.

5 Reduced-Order Single-Axis Models

The previous sections provide several models of the 4th-order plant, emphasizing the interactions between link 1 and link 2. The nonlinear model of §2 is useful as a high-fidelity model for simulation purposes or for nonlinear controller design purposes, whereas the linear models of §3 and §4 are intended for linear analysis and design. In certain applications, both the design of controllers and the shaping of reference commands will be simplified by modeling the motions of link 1 and link 2 as independent and non-interacting 2nd-order subsystems. Such reduced-order single-axis models are necessarily approximate, but in some circumstances such approximations are well motivated.

Single-axis model for rotation about vertical axis: Suppose that $\theta_2 = 0$ or $\theta_2 = \pi$ for all $t \geq 0$, which suggests that link 0, link 1 and link 2 are rigidly connected and their combination represents a lumped inertial load for rotation about the vertical axis. Under this scenario, (2) indicates that the vertical axis rotations would be modeled with torque input by

$$\left(J_0 + J_1 + m_2 L_1^2\right)\ddot{\theta}_1 + d_1\dot{\theta}_1 = \tau.$$

For the case of voltage input, use of (1) yields the modified result

$$\left(J_0 + J_1 + m_2 L_1^2\right)\ddot{\theta}_1 + \left(d_1 + K_m^2/R_m\right)\dot{\theta}_1 = \left(K_m/R_m\right)v.$$

To summarize, vertical axis rotations are modeled by

$$\dot{\xi}_1 = \begin{bmatrix} 0 & 1 \\ 0 & -\alpha \end{bmatrix}\xi_1 + \begin{bmatrix} 0 \\ \beta \end{bmatrix}u \tag{8}$$

$$y = \begin{bmatrix} 1 & 0 \end{bmatrix}\xi_1 \tag{9}$$

where the signals are

$$\xi_1 = \begin{bmatrix} \theta_1 \\ \dot{\theta}_1 \end{bmatrix}, \quad u = \begin{cases} \tau & \text{, torque input} \\ v & \text{, voltage input} \end{cases}$$

and the coefficients are

$$\alpha = \begin{cases} \dfrac{d_1}{J_0 + J_1 + m_2 L_1^2} & \text{, torque input} \\ \dfrac{d_1 + K_m^2/R_m}{J_0 + J_1 + m_2 L_1^2} & \text{, voltage input} \end{cases}, \quad \beta = \begin{cases} \dfrac{1}{J_0 + J_1 + m_2 L_1^2} & \text{, torque input} \\ \dfrac{K_m/R_m}{J_0 + J_1 + m_2 L_1^2} & \text{, voltage input.} \end{cases}$$

Single-axis model for rotation about horizontal axis: Suppose that θ_1 is constant (at any value) for all $t \geq 0$, in which case the only motion is un-driven rotation of link 2 about the horizontal axis. Under this scenario, (2) indicates that the horizontal axis rotations would be modeled by

$$J_2\ddot{\theta}_2 + d_2\dot{\theta}_2 + m_2 g l_2 \sin\theta_2 = 0$$

which is the classic pendulum equation. Linearization about either equilibrium point yields

$$\dot{\xi}_2 = \begin{bmatrix} 0 & 1 \\ \pm m_2 g l_2/J_2 & -d_2/J_2 \end{bmatrix}\xi_2 \tag{10}$$

where the upper/lower sign on the coefficient is used for the up/down equilibrium and

$$\xi_2 = \begin{bmatrix} \theta_2 - \theta_{2,\text{eq}} \\ \dot{\theta}_2 \end{bmatrix}, \quad \theta_{2,\text{eq}} = \begin{cases} \pi & \text{, up equilibrium} \\ 0 & \text{, down equilibrium.} \end{cases}$$

6 Determining Parameter Values

In a previous lab project, we learned that parameter identification methods are available that can automate the process of extracting unknown plant parameter values from measured input-output responses. Here we will take another approach to estimate plant parameter values, in order to help understand how mass and inertia are modeled. We are seeking the parameter values listed in Figure 1b, and we will use inertia formulas from the following websites:

- `https://en.wikipedia.org/wiki/List_of_moments_of_inertia`;
- `https://en.wikipedia.org/wiki/Parallel_axis_theorem`.

Some parameter values are listed in a table provided by Quanser, but separate measurements were made to confirm and/or supplement the listed values.

Link 0

For link 0, the inertia J_0 is obtained by summing three inertia values:

$$J_0 = J_{0,\text{rotor}} + J_{0,\text{hub}} + J_{0,\text{housing}}.$$

Two of these inertia values have been tabulated:

$$J_{0,\text{rotor}} = 4 \times 10^{-6} \text{ kg m}^2, \quad J_{0,\text{hub}} = 0.6 \times 10^{-6} \text{ kg m}^2.$$

The remaining inertia value must be approximated because the housing's mass distribution is not precisely known. One possibility is to assume that the housing is a solid cylinder, in which case

$$J_{0,\text{housing}} = \tfrac{1}{12} m_{0,\text{housing}} \left(3r_{0,\text{housing}}^2 + L_{0,\text{housing}}^2\right). \tag{11}$$

Another possibility is to assume that the housing is a thin cylinder, in which case

$$J_{0,\text{housing}} = \tfrac{1}{12} m_{0,\text{housing,s}} \left(6r_{0,\text{housing}}^2 + L_{0,\text{housing}}^2\right) + \tfrac{1}{2} m_{0,\text{housing,e}} \left(r_{0,\text{housing}}^2 + L_{0,\text{housing}}^2\right) \tag{12}$$

where the surface (s) and end (e) mass fractions are

$$m_{0,\text{housing,s}} = \frac{m_{0,\text{housing}} L_{0,\text{housing}}}{r_{0,\text{housing}} + L_{0,\text{housing}}}, \quad m_{0,\text{housing,e}} = \frac{m_{0,\text{housing}} r_{0,\text{housing}}}{r_{0,\text{housing}} + L_{0,\text{housing}}}.$$

The required data for evaluation of $J_{0,\text{housing}}$ are the approximate measured values

$$m_{0,\text{housing}} = 0.067 \text{ kg}, \quad L_{0,\text{housing}} = 0.038 \text{ m}, \quad r_{0,\text{housing}} = 0.014 \text{ m}.$$

The values of $J_{0,\text{housing}}$ obtained from (11) and (12) vary significantly. Since the dominant term in J_0 is $J_{0,\text{housing}}$, there is uncertainty in J_0. On the other hand, J_0 is not the dominant term in J_{11}, so uncertainty in J_0 is unlikely to cause problems. We will use the thin cylinder assumption.

Link 1

For link 1, the mass value is measured as

$$m_1 = 0.025 \text{ kg}.$$

Link 1 is characterized by the measured lengths

$$L_{1,\text{total}} = 0.11 \text{ m}, \quad L_{1,\text{offset}} = 0.02 \text{ m}$$

from which we determine the center of mass location

$$l_1 = \tfrac{1}{2} L_{1,\text{total}} - L_{1,\text{offset}}.$$

The inertia values are determined from a thin-rod assumption:

$$I_1 = \tfrac{1}{12} m_1 L_{1,\text{total}}^2, \quad J_1 = I_1 + m_1 l_1^2.$$

Link 2

For link 2, the mass value is measured as

$$m_2 = 0.024 \text{ kg}.$$

Link 2 is characterized by the measured lengths

$$L_{2,\text{total}} = 0.129 \text{ m}, \quad L_{2,\text{offset}} = 0.008 \text{ m}$$

from which we determine the center of mass location

$$l_2 = \tfrac{1}{2}L_{2,\text{total}} - L_{2,\text{offset}}.$$

The inertia values are determined from a thin-rod assumption:

$$I_2 = \tfrac{1}{12}m_2 L_{2,\text{total}}^2, \quad J_2 = I_2 + m_2 l_2^2.$$

Other

The measured distance between the rotation axes is

$$L_1 = 0.085 \text{ m}.$$

The acceleration due to gravity is

$$g = 9.81 \text{ m/s}^2.$$

The motor magnetic coefficient and resistance are listed as

$$K_m = 0.042 \text{ Nm/A}, \quad R_m = 8.4\ \Omega.$$

The viscous friction coefficients are coarsely approximated as

$$d_1 = 10^{-3} \text{ Nm s}, \quad d_2 = 10^{-5} \text{ Nm s}.$$

Mass Measurements

The moving components consist of link 0, link 1, and link 2, where link 0 and link 1 are rigidly connected. Link 1 is a solid steel shaft. Figure 3a shows four copies of link 1 having a mass of 0.100 kg. Therefore, the measured mass value for link 1 is

$$m_1 = 0.025 \text{ kg}.$$

Link 2 is a solid aluminum shaft. Figure 3b shows three copies of link 2 having a mass of 0.072 kg. Therefore, the measured mass value for link 2 is

$$m_2 = 0.024 \text{ kg}.$$

Link 0 consists of four parts; the motor's rotor, the attachment hub, the bearing housing, and the encoder housing. The masses of the first two parts (in the base) have not been measured, but their inertia values were listed in a data sheet. The bearing housing (red) has much larger mass than the encoder housing (black), due to the materials used to construct these housings; these two parts are collectively referred to as the housing. The housing mass is estimated from the overall mass of three parts; the partial mass of link 0 (not including the motor's rotor or the attachment hub, but including the encoder cable), the mass of link 1, and the mass of link 2. Using the measurement shown in Figure 3c, the mass of the housing portion of link 0 is estimated to be

$$m_{0,\text{housing}} = 0.116 - 0.025 - 0.024 = 0.067 \text{ kg}.$$

The above mass measurements were used to determine various plant model coefficients.

(a) Link 1 copies. (b) Link 2 copies. (c) Links 0 (portion), 1 and 2.

Figure 3: Mass measurements of the pendulum attachment and its components.

7 Model Analysis in Matlab

The linear models of §4 are accessible in the Matlab script `qms_model.m` which is available on Canvas; the listing of this script is displayed below. Both equilibrium cases are supported, down for the crane application and up for the rocket application. Only the voltage input case is supported, but it would be simple to add the torque input case if needed. This script uses the same parameter values discussed earlier in this document. At the end of this script, the plant model is provided in terms of its coefficient matrices (A, B, C), its transfer function $P(s)$, and its pole and zero locations. The results are shown in Figures 4/5 for the down/up equilibrium cases.

```
% David Taylor, Georgia Tech, 7/12/23

clc, clear, close all
format shortE

%% settings (1 = yes, 0 = no)

% use 0 for model of crane plant
% use 1 for model of rocket plant

pendulum_up = 0;

%% link 0

J0_rotor = 4e-6;
```



```
J0_hub = 0.6e-6;

m0_housing = 0.067;
L0_housing = 0.038;
r0_housing = 0.014;

m0_housing_s = m0_housing*L0_housing/(r0_housing+L0_housing);
m0_housing_e = m0_housing*r0_housing/(r0_housing+L0_housing);
J0_housing_s = (1/12)*m0_housing_s*(6*r0_housing^2+L0_housing^2);
J0_housing_e = (1/2)*m0_housing_e*(r0_housing^2+L0_housing^2);
J0_housing = J0_housing_s+J0_housing_e;

J0 = J0_rotor+J0_hub+J0_housing;

%% link 1

m1 = 0.025;
L1_total = 0.11;
L1_offset = 0.02;
l1 = 0.5*L1_total-L1_offset;
I1 = (1/12)*m1*L1_total^2;
J1 = I1+m1*l1^2;

%% link 2

m2 = 0.024;
L2_total = 0.129;
L2_offset = 0.008;
l2 = 0.5*L2_total-L2_offset;
I2 = (1/12)*m2*L2_total^2;
J2 = I2+m2*l2^2;

%% other

L1 = 0.085;
g = 9.81;
Km = 0.042;
Rm = 8.4;
d1 = 1e-3;
d2 = 1e-5;

%% plant model parameters (voltage input)

J11 = J0+J1+m2*L1^2;
J12 = m2*L1*l2;
J21 = J12;
J22 = J2;
T22 = m2*g*l2;
```



```
den = J11*J22-J12*J21;

if pendulum_up == 1
    a32 = J12*T22/den;
    a33 = -J22*(d1+Km^2/Rm)/den;
    a34 = -J12*d2/den;
    a42 = J11*T22/den;
    a43 = -J21*(d1+Km^2/Rm)/den;
    a44 = -J11*d2/den;
    b3 = (J22*Km/Rm)/den;
    b4 = (J21*Km/Rm)/den;
else
    a32 = J12*T22/den;
    a33 = -J22*(d1+Km^2/Rm)/den;
    a34 = J12*d2/den;
    a42 = -J11*T22/den;
    a43 = J21*(d1+Km^2/Rm)/den;
    a44 = -J11*d2/den;
    b3 = (J22*Km/Rm)/den;
    b4 = -(J21*Km/Rm)/den;
end

%% full-order plant model (voltage input)

A = [0,0,1,0;0,0,0,1;0,a32,a33,a34;0,a42,a43,a44]
B = [0;0;b3;b4]
C = [1,0,0,0]

P = tf(ss(A,B,C,0))
[P_zeros,P_poles,P_gain] = zpkdata(P,'v')
```

```
A =

           0            0   1.0000e+00            0
           0            0            0   1.0000e+00
           0   1.0079e+02  -8.7409e+00   7.5765e-02
           0  -2.2675e+02   9.1676e+00  -1.7046e-01

B =

           0
           0
   3.6120e+01
  -3.7883e+01

C =

     1     0     0     0

P =

       36.12 s^2 + 3.287 s + 4372
  -----------------------------------
  s^4 + 8.911 s^3 + 227.5 s^2 + 1058 s

Continuous-time transfer function.

P_zeros =

  -4.5498e-02 + 1.1002e+01i
  -4.5498e-02 - 1.1002e+01i

P_poles =

   0.0000e+00 + 0.0000e+00i
  -1.9134e+00 + 1.4298e+01i
  -1.9134e+00 - 1.4298e+01i
  -5.0846e+00 + 0.0000e+00i

P_gain =

   3.6120e+01
```

Figure 4: Voltage input 4th-order model corresponding to pendulum down equilibrium.

```
A =

           0            0   1.0000e+00            0
           0            0            0   1.0000e+00
           0   1.0079e+02  -8.7409e+00  -7.5765e-02
           0   2.2675e+02  -9.1676e+00  -1.7046e-01

B =

           0
           0
  3.6120e+01
  3.7883e+01

C =

     1     0     0     0

P =

     36.12 s^2 + 3.287 s - 4372
  ---------------------------------
  s^4 + 8.911 s^3 - 226 s^2 - 1058 s

Continuous-time transfer function.

P_zeros =

 -1.1048e+01
  1.0957e+01

P_poles =

           0
  1.3543e+01
 -1.8149e+01
 -4.3048e+00

P_gain =

  3.6120e+01
```

Figure 5: Voltage input 4th-order model corresponding to pendulum up equilibrium.